about 1.3. Of course, as α decreases, the resultant velocity ratio decreases. With the materials considered here, if α is decreased below about $\frac{1}{4}$, the velocity advantage begins to disappear.

In conclusion, when maintenance of moderate wall temperatures is required, it appears that condensation in a supersonic nozzle is a promising way of increasing exit velocity (specific impulse) for propulsion units.

References

[1] Wegener, P. G. and Mack, L. M., "Condensation in Supersonic and Hypersonic Wind Tunnels," *Advances in Applied Mechanics*, Vol. V, Academic Press, New York, 1958, pp. 307–447.

[2] Norgren, C. T., "On Board Colloidal Particle Generator for Electrostatic Engines," *AIAA Progress in Astronautics and Aeronautics: Electric Propulsion Development*, Vol. 9, edited by E. Stuhlinger, Academic Press, New York, 1963, pp. 407–434.

[3] Goldin, D. S., "A Thermodynamic Flow Analysis of Particle Formation Efficiency in a Mixed Flow Colloidal Thrustor," AIAA Paper 67-85, New York, 1967.

[4] Cox, A. L., "Colloidal Electrohydrodynamic Energy Converter," *AIAA Journal*, Vol. 1, No. 11, Nov. 1963, pp. 2491–2497.

[5] Shapiro, A. H., *Dynamics and Thermodynamics Compressible Fluid Flow*, Ronald Press, New York, 1953.

[6] Sherman, P. M., McBride, D. D., Chmielewski, T., Pierce, T. H., and Oktay, E., "Condensation of Metal Vapor in a Supersonic Carrier Gas," USAF OAR ARL-69-0089, June 1969, U.S. Air Force.

[7] McBride, D. D. and Sherman, P. M., "A Solution for Equilibrium Condensation on Two Component Flow Through a Nozzle," *Astronautica Acta*, Vol. 16, 1970.

[8] Chmielewski, T. and Sherman, P. M., "The Effect of a Carrier Gas on Homogeneous Condensation in a Supersonic Nozzle," *AIAA Journal*, Vol. 8, No. 4, April 1970, pp. 798–893.

Population Inversions behind Normal Shock Waves

JOHN D. ANDERSON JR.* AND MICHAEL T. MADDEN†
U. S. Naval Ordnance Laboratory, White Oak, Md.

Introduction

As early as 1962, Basov and Oraevskii[1] suggested that population inversions in molecular systems could be created by rapid heating or cooling of the system. Subsequently, Hurle and Hertzberg[2] suggested that population inversions could be obtained in the rapid, nonequilibrium expansion of an initially hot gas through a supersonic nozzle. Indeed, experimental and theoretical results for such inversions, as well as laser stimulated emission, have been recently obtained in expansions of CO_2–N_2–He or H_2O mixtures (see the reviews in Refs. 3–5).

In contrast to rapid cooling, the present Note describes a theoretical study of vibrational population inversions created by rapid heating behind a normal shock wave in CO_2–N_2–He mixtures. On one hand, the creation of population inversions behind normal shock waves by means of shock-initiated chemical reactions have been studied by Oraevskii[6] and Gross et al.[7] Here, the inversions are formed directly by the preferential conversion of chemical energy into electronic[6] or vibrational[7] energy of the product species; this is the general principle of chemical lasers. On the other hand, the present Note examines the purely vibrational relaxation processes behind a normal shock wave in CO_2–N_2–He mixtures. The results of this analysis indicate that population inversions between the (200) and (001), and between the (04°0) and (001) vibrational energy levels of CO_2, can be created by molecular vibrational energy exchange only. Moreover, the present Note assesses the potential of this nonequilibrium flow as a possible laser medium.

Received October 22, 1970; revision received March 4, 1971. This work was supported by the NOL Independent Research Program.

* Chief, Hypersonics Group, Aerophysics Division. Member AIAA.

† Aerospace Engineer, Aerophysics Division. Associate Member AIAA.

Vibrational Model

The vibrational model assumed for the present study is shown in Fig. 1, which contains the pertinent low-lying vibrational energy levels of CO_2 and N_2. This model is described in detail in Ref. 8; in essence, the participating energy levels are grouped into modes I and II which are assumed in equilibrium within themselves, but not with each other. The net vibrational energies per unit mass, e_{vib_I} and $e_{vib_{II}}$, are the dependent nonequilibrium variables, which are assumed to relax according to the equations

$$\dot{w}_I = d(e_{vib})_I/dt = (1/\tau_I)[(e_{vib})_I^{eq} - (e_{vib})_I] \quad (1)$$

$$\dot{w}_{II} = d(e_{vib})_{II}/dt = (1/\tau_{II})[(e_{vib})_{II}^{eq} - (e_{vib})_{II}] \quad (2)$$

Here, τ_I and τ_{II} are the characteristic relaxation times for modes I and II, respectively; they are averages which depend on τ_a, τ_b, and τ_c for the mixture (see Fig. 1).

This vibrational model is a reasonable *approximation* for the detailed translation-vibration (T-V) and vibration-vibration (V-V) energy transfers within the CO_2–N_2–He mixture. Details of the approximations and their justification are as follows: 1) The relaxation (excitation) of mode I is assumed to be governed by the T-V transfer, τ_c. This is justified because the much slower V-V transfer, τ_a, has only a weak influence on mode I. For example, for a mixture of 60% He, 1.9% CO_2 and 38.1% N_2 at room temperature, the data of Ref. 9 show $\tau_a/\tau_c = 24$. Obviously, for the mixtures of interest here, τ_c is the prevailing relaxation time for the net excitation of mode I. 2) For the relaxation of mode II, both T-V and V-V energy exchanges are taken into account through the use of both τ_a and τ_b in the calculation of τ_{II} (see Ref. 8). With this value of τ_{II}, MacDonald[10] has kindly pointed out that Eq. (2) becomes more precise as T_{vib_I} approaches the gas translational temperature, T. For the case of present interest, this condition prevails; mode I relaxes very rapidly and is reasonably equilibrated with T before most of the mode II relaxation takes place. This behavior has been clearly established in both experimental and theoretical

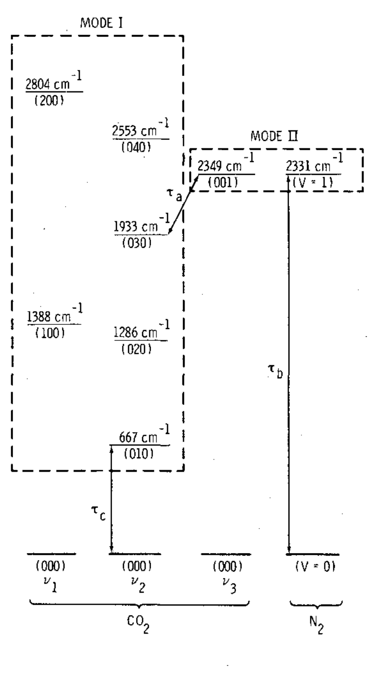

Fig. 1 Vibrational model.

studies of gasdynamic lasers employing CO_2–N_2–He or H_2O mixtures.[3–5] 3) The accuracy of the present vibrational model has been substantiated by numerous comparisons with experiment. For example, Fig. 2 illustrates the variation of small-signal laser gain (which is proportional to population inversion) in a rapidly expanding gas as a function of distance through a supersonic nozzle and a downstream constant area duct. The experimental data were measured in the NOL 3-Megawatt Arc Tunnel[5]; the theoretical results were obtained from the analysis of Ref. 8 using the same vibrational model as employed in the present Note. Excellent agreement is obtained. At large distances downstream of the nozzle exit, the experimental data drops slightly below the theoretical curve due to weak shock waves and other viscous effects in the experimental flow. Independently, Lee[11] has also found excellent agreement between his arc tunnel gasdynamic laser experiments (using CO_2–N_2–He mixtures) and the analysis of Ref. 8. Moreover, the present vibrational model yields small-signal gain predictions which are in reasonable agreement with shock tunnel experiments[12] for CO_2–N_2–He mixtures. These comparisons, among others, promote substantial confidence in the present model.

Finally, emphasis is made that the model in its present form is formulated only for the calculation of population inversions in CO_2–N_2–He or H_2O mixtures; it is not necessarily valid for other gases, nor can it be used when substantial amounts of radiative power is being extracted from the flow.

Analysis

The present gas dynamic analysis makes the standard assumptions of a stationary, discontinuous shock front with frozen conditions immediately behind the front. Hence, at this location ρ_2, T_2, and u_2 are obtained from the standard calorically perfect gas equations for normal shocks, and e_{vib_I} and e_{vib_II} are equal to their respective upstream values. In turn, these quantities are the boundary conditions for the downstream nonequilibrium flow, which is solved by forward numerical integration of the governing steady flow conservation equations as functions of distance behind the shock front. These equations are:

$$\text{Continuity:} \quad u d\rho/dx + \rho du/dx = 0 \tag{3}$$

$$\text{Momentum:} \quad (RT/\rho)d\rho/dx + RdT/dx + udu/dx = 0 \tag{4}$$

$$\text{Energy:} \quad RTdu/dx + uR\alpha dT/dx + ud/dx(e_{\text{vib}_\text{I}} + e_{\text{vib}_\text{II}}) = 0 \tag{5}$$

$$\text{Rate:} \quad de_{\text{vib}_\text{I}}/dx = \dot{w}_\text{I}/u \text{ and } de_{\text{vib}_\text{II}}/dx = \dot{w}_\text{II}/u \tag{6}$$

where $\alpha = \frac{3}{2}X_{He} + \frac{5}{2}(X_{CO_2} + X_{N_2})$, $p = \rho RT$, and the notation is standard. The solution is terminated when equilibrium values of the normal shock properties are closely approached; equilibrium normal shock properties for CO_2–N_2–He mixtures are known in advance from Ref. 13. A detailed discussion of the numerical aspects of the present study can be found in Ref. 14.

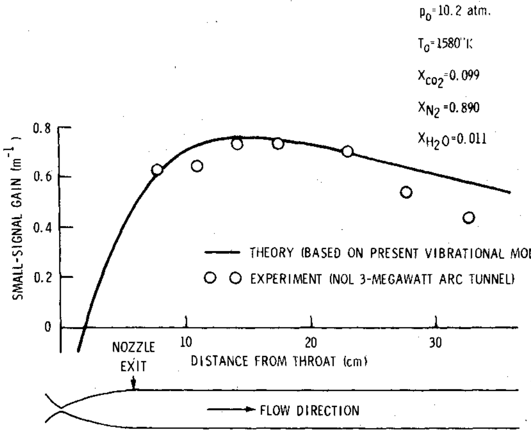

Fig. 2 Profile of gasdynamic laser gain for a minimum length contoured nozzle (throat height = 1 mm and inviscid area ratio = 20) exhausting into a constant area duct.

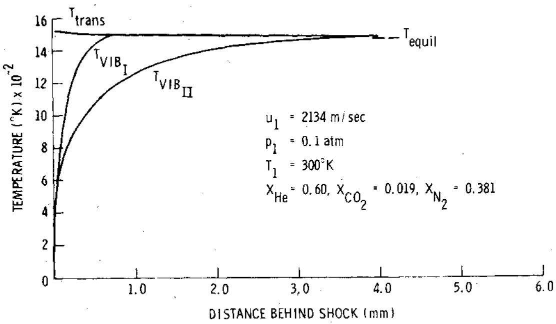

Fig. 3 Variation of translational and vibrational temperature behind the shock front.

Results

Numerical results for a typical case are shown in Figs. 3 and 4. Figure 3 illustrates temperature variations in the nonequilibrium region behind the shock front, and clearly shows the rapid equilibration of T_{vib_I} with the translational temperature T, whereas in contrast, T_{vib_II} relaxes more slowly. At a distance of 4 mm downstream of the shock front, all three temperatures have equilibrated within one percent of the final equilibrium temperature, which has been taken from the results of Ref. 13. The results shown in Fig. 3 reflect a molecular collisional process which indeed leads to population inversions behind the shock front, as shown in Fig. 4. These inversions occur between the (04°0) and (001) levels and to a lesser degree between the (200) and (001) levels in CO_2. Examining Fig. 4, near the shock front the inversions rapidly increase due to the rapid population of the excited levels of mode I while at the same time the excitation of mode II is lagging far behind. However, the inversion soon peaks and begins to decrease farther downstream as the lower (001) level is substantially populated. Note that, for the given upstream conditions, the inversions persist over a length from 1–2 mm behind the shock front. The vibrational kinetics obey binary scaling; hence, the spatial extent of the population inversions can be increased or decreased by a proportional decrease or increase in p_1, keeping T_1 and u_1 the same. Many additional results obtained from the present study are discussed in Ref. 14.

Discussion

How do the laser properties of this nonequilibrium shock flow compare with those obtained by rapid expansions?

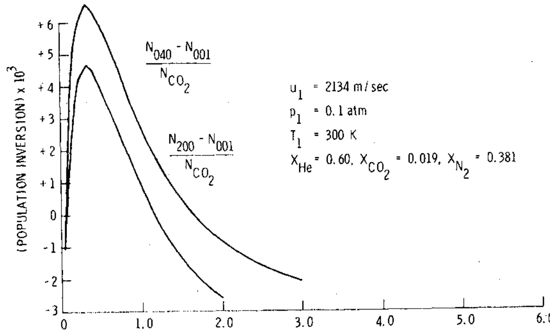

Fig. 4 Variation of population inversions behind the shock front.

First, the conventional, rapid expansion gas dynamic laser[3-5] creates a population inversion between the (001) and (100) levels in CO_2 which subsequently lases at $\lambda = 10.6\mu$. In contrast, the inversions shown in Fig. 4 between the (04°0) and (001) levels, and between the (200) and (001) levels, would correspond to laser transitions at 50μ and 22μ, respectively. An important parameter for gas lasers is small signal gain, G_0, defined as $dI/I = G_0dz$ where I is the incident radiation intensity on a slab of laser gas of thickness dz, and dI is the increase in beam intensity after traversing the length dz. As shown in Appendix A of Ref. 15, $G_0 \propto (\lambda^2/\tau_{21})\cdot IN \propto (M^2/\lambda)\cdot IN$, where τ_{21} is the spontaneous radiative lifetime for a transition between the upper and lower laser levels, M is the corresponding quantum mechanical matrix element, and IN is the population inversion. For CO_2, computed values of M for the 50μ, 22μ, and 10.6μ transitions are in the ratio 0.21×10^{-2}:0.21×10^{-2}:0.34×10^{-1}, respectively.[16] Also, the shock induced population inversions shown in Fig. 4 are approximately one order of magnitude smaller than typical inversions created in rapid expansions through supersonic nozzles. In light of the above numbers, a comparison of G_0 at 50μ and 22μ behind a shock wave with G_0 at 10.6μ in a rapid expansion leads to $(G_0)_{50\mu}/(G_0)_{10.6\mu} \approx 10^{-4}$ and $(G_0)_{22\mu}/(G_0)_{10.6\mu} \approx 2 \times 10^{-4}$. Clearly, the nonequilibrium region behind a normal shock wave in CO_2–N_2–He mixtures produces a low-gain medium. A more detailed discussion and comparison of these and other laser properties are contained in Ref. 14.

Conclusion

The present study indicates that population inversions occur behind a normal shock front due strictly to translation-vibration and vibration-vibration molecular energy exchanges in CO_2–N_2–He mixtures. However, the laser properties of this shock-induced nonequilibrium flow are clearly not as promising as those of gas dynamic lasers operating on the principle of rapid expansion.

References

[1] Basov, N. G. and Oraevskii, A. N., "Attainment of Negative Temperatures by Heating and Cooling of a System," *Soviet Physics JETP*, Vol. 17, No. 5, Nov. 1963, pp. 1171–1172.

[2] Hurle, I. R. and Hertzbeg, A., "Electronic Population Inversions by Fluid—Mechanical Techniques," *The Physics of Fluids*, Vol. 8, No. 9, Sept. 1965, pp. 1601–1607.

[3] Gerry, E. T., "Gasdynamic Lasers," AIAA Paper 71-23, New York, 1971.

[4] Hertzberg, A. et al., "Photon Generators and Engines for Laser Power Transmission," AIAA Paper 71-106, New York, 1971.

[5] Anderson, J. D., Jr. and Winkler, E. M., "High Temperature Aerodynamics with Electromagnetic Radiation," *Proceedings of the IEEE*, Vol. 59, No. 4, April 1971, pp. 651–658.

[6] Oraevskii, A. N., "Population Inversion Obtained by Thermal Dissociation of Molecules in a Shock Wave," *Soviet Physics JETP*, Vol. 21, No. 4, Oct. 1965, pp. 768–770.

[7] Gross, R. W. F. et al., "Stimulated Emission Behind Overdriven Detonation Waves in F_2O-H_2 Mixtures," *Journal of Chemical Physics*, Vol. 51, No. 3, Aug. 1969, p. 1250.

[8] Anderson, J. D., Jr., "A Time-Dependent Analysis of Population Inversions in an Expanding Gas," *The Physics of Fluids*, Vol. 13, No. 8, Aug. 1970, pp. 1983–1989.

[9] Taylor, R. L. and Bitterman, S., "Survey of Vibrational Relaxation Data for Processes Important in the CO_2–N_2 Laser System," *Reviews of Modern Physics*, Vol. 41, No. 1, Jan. 1969, pp. 26–47.

[10] MacDonald, J. R., private communication, Jan. 20, 1971, Max-Planck-Institut Fur Plasmaphysik, Garching Bei Munchen, West Germany.

[11] Lee, G. and Gowan, F. E., "Gain of CO_2 Gasdynamic Lasers," *Applied Physics Letters*, Vol. 18, No. 6, March 15, 1971, pp. 237–239.

[12] Christiansen, W. H., and Tsongas, G. A., "Gain Kinetics of High Pressure Gasdynamic Lasers," Univ. of Washington (submitted for publication in *The Physics of Fluids*).

[13] Madden, M. T., Anderson, J. D., Jr., and Piper, C. H., "Equilibrium Normal Shock Properties for Vibrationally Excited CO_2–N_2–He Mixtures," NOLTR 70-103, May 1970, U.S. Naval Ordnance Lab., White Oak, Md.

[14] Anderson, J. D., Jr., Madden, M. T., and Piper, C. H., "Vibrational Population Inversions Behind Normal Shock Waves in CO_2–N_2–He Mixtures," NOLTR 70-214, Oct. 1970, U. S. Naval Ordnance Lab., White Oak, Md.

[15] Anderson, J. D., Jr., "Numerical Experiments Associated with Gas Dynamic Lasers," NOLTR 70-198, Sept. 1970, U.S. Naval Ordnance Lab., White Oak, Md.

[16] Lalos, G., private communication, Aug. 6, 1970, U.S. Naval Ordnance Lab., White Oak, Md.

Computation of Incompressible Turbulent Boundary Layers at Low Reynolds Numbers

TUNCER CEBECI* AND G. J. MOSINSKIS†

Douglas Aircraft Company, Long Beach, Calif.

Introduction

CURRENTLY there are several quite accurate numerical methods for calculating turbulent boundary layers. Some of these methods are based on the solution of the momentum integral and/or energy integral equations and are called integral methods. Other methods are based on the solution of the governing conservation equations in their partial-differential equation form. These are called differential methods. Almost all these prediction methods are based on empirical data obtained at high Reynolds numbers ($R_\theta >$ 6000). According to several experiments and investigators there is a definite Reynolds effect for $R_\theta < 6000$. For example, in Ref. 1, Coles observed that his law of the wall formulation failed for low Reynolds numbers; the strength of the wake component, which stayed constant for momentum Reynolds numbers greater than 6000, showed a large variation at low Reynolds numbers. It should, however, be mentioned that Coles' analysis relies on the constancy of k and c in the logarithmic velocity profile.

$$u^+ \equiv u/u_\tau = 1/k \ln(yu_\tau/\nu) + c, \quad u_\tau \equiv (\tau_w/\rho)^{1/2} \qquad (1)$$

The low Reynolds number effect is quite important in turbomachines and on airfoils in wind tunnels. For example,

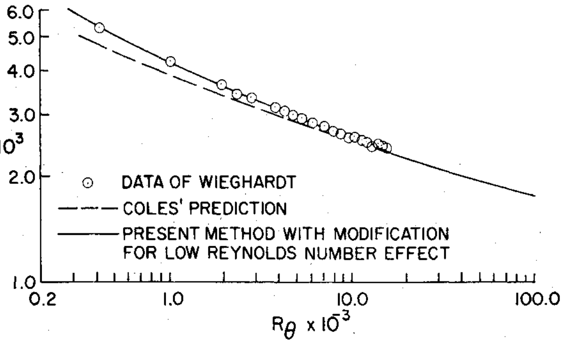

Fig. 1 Calculated and experimental skin-friction coefficients for a flat-plate turbulent flow at low Reynolds numbers.

Received February 8, 1971; revision received March 29, 1971. This research was supported by the Naval Ship Research and Development Center under Contract N00014-70-C-0099, Subproject SR 009 01 01.

Index Category: Boundary Layers and Convective Heat Transfer-Turbulent.

* Senior Engineer/Scientist, Aerodynamics Research. Member AIAA.

† Engineer/Scientist, Aerodynamics Research. Member AIAA.